Spherical Spiral Scanning for Automotive Antenna Measurements

Jeffrey A. Fordham
MI Technologies
1125 Satellite Blvd, Suite 100, Suwanee, GA 30024

Francesco D'Agostino
D.I.In. University of Salerno, via Giovanni Paolo II,132, I-84084 Fisciano (SA), Italy

Abstract— **Spherical spiral scanning involves coordinating the motion of two simultaneous axes to accomplish near-field antenna measurements along a line on a sphere that does not cross itself. The line would ideally start near a pole and trace a path along the sphere to the other pole. An RF probe is moved along this path in order to collect RF measurements at predefined locations. The data collected from these measurements is used along with a near-field to far-field transformation algorithm to determine the radiated far-field antenna pattern.**

The method for transforming data collected along a spherical spiral scan has been previous presented [12, 13]. Later laboratory measurement studies have shown the validity of the technique [23].

A review of the spherical spiral scanning technique and its recent advances, resulting from about ten years of research collaboration between the UNISA Antenna Characterization Research Group and MI Technologies is here presented. Such a scan technique relies on the non-redundant sampling representations of EM fields and takes full advantage of moving two axes simultaneously. Accordingly, it allows one to drastically reduce the overall number of required data and the time to collect the data. This scanning technique can be properly applied in testing antennas mounted on automobiles in order to reduce the overall time of the measurement.

Keywords: Spherical Near-Field, Telematics, Automotive

I. INTRODUCTION

The near-field – far-field (NF–FF) transformation techniques have assumed a significant role in modern antenna measurements [1-5], since they overcome all drawbacks which make impractical the radiation pattern measurement of electrically large antennas in a conventional FF range. Among these techniques, a spherical near field (SNF) scan is particularly attractive because it avoids the errors due to the truncation of the scanning surface, thus allowing the reconstruction of the whole radiation pattern of the antenna under test (AUT). Therefore, SNF has attracted considerable interest over the years [6-13].

NF–FF transformation techniques that use a spiral mapped over the spherical surface have been recently proposed [15-18]. Such spiral scanning is now possible with the latest position control systems. By exploiting continuous and synchronized movements of the positioning systems of the probe and AUT, significant reduction in the measurement time is possible. These techniques rely on the non-redundant sampling representations of electromagnetic (EM) fields [19, 20] and employ optimal sampling interpolation (OSI) formulas [21] to efficiently recover the NF data in a format required by the classical spherical NF–FF transformation [10]. The modification has been described in earlier work [12, 13]. In particular, the non-redundant sampling representation on the sphere from samples collected along the spiral and the related OSI expansion have been developed in [15, 16] by assuming the AUT as enclosed in the smallest sphere able to contain it and choosing the spiral step equal to the sample spacing required for the interpolation along a meridian. Then, NF–FF transformations with spherical spiral scanning tailored for electrically long or quasi-planar antennas have been proposed in [17, 18] by properly applying the unified theory of spiral scans for non-spherical antennas [22]. In particular, a prolate and an oblate ellipsoid have been adopted in [17] to model an elongated and a quasi-planar antenna, respectively. Whereas in [18], an elongated AUT has been considered as enclosed in a cylinder ended in two half spheres, and a surface formed by two circular bowls with the same aperture diameter but different lateral bends has been used for modelling quasi-planar antennas. The experimental validity of all these NF-FF transformation techniques have been more recently assessed in the references [23-27]. It has been shown that, although these techniques allow drastic reductions in the number of NF data and the time needed for their measurement, the same accuracy as the standard transformation technique [10] is retained.

Figure 1 shows a spherical near field measurement system example for testing antennas mounted on large vehicles using classical SNF sampling. In this system the vehicle turntable is rotated continuously while the RF probe is stepped along the arch shown in the figure. The probe is successively moved to an equally spaced set of points along the theta axis (arch) while data is collected rapidly along the phi (turntable) axis. This method of collecting a data set results in equal increments along both the theta and phi axes. This type of spherical near-field scanning has been described by Hansen [10]. In his book Hansen included the mathematics behind the spherical wave expansion to transform data collected on the measurement sphere to those fields as they exist in the far-field region.

In this work, we present recent advances resulting from about ten years of research collaboration between UNISA Antenna Characterization Research Group and MI Technologies, which has concerned the spiral NF scanning techniques too. Moreover,

we propose to apply the non-redundant spherical spiral scan technique based on the oblate [12, 18] ellipsoidal modelling to the testing of antennas mounted on automobiles, in order to achieve in such a case a reduction in the number of data points and in the time required for their acquisition.

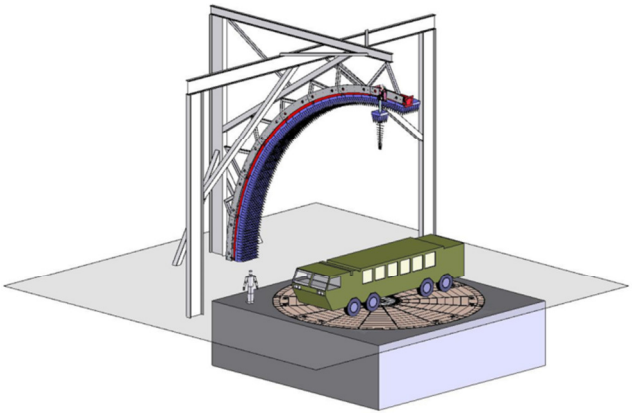

Figure 1: A SNF system for measuring antennas mounted on large vehicles.

II. Nonredundant Voltage Representation on a Sphere

Let us consider a quasi-planar AUT enclosed in an oblate ellipsoid Σ having major and minor semi-axes equal to a and b, a nondirective probe scanning a proper spiral lying on a sphere of radius d in the NF region, and adopt the spherical coordinate system (r, ϑ, φ) to denote an observation point P (Figure 2).

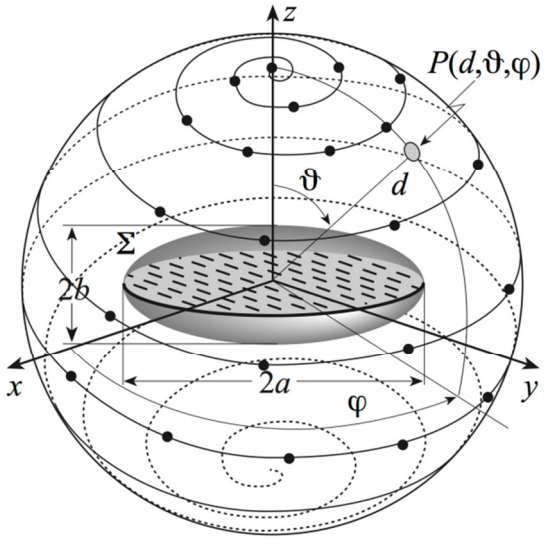

Figure 2: Spherical spiral scanning for a quasi-planar AUT.

Since the voltage V measured by such a probe has the same effective spatial bandwidth of the field [23], the non-redundant representations of EM fields [14] can be applied to it. Accordingly, when dealing with the representation on a curve C, it is convenient to adopt a proper analytical parameterization $\underline{r} = \underline{r}(\eta)$ to describe C and to introduce the "reduced voltage"

$$\tilde{V}(\eta) = V(\eta)\, e^{j\psi(\eta)}\,, \tag{1}$$

where V is the voltage V_1 or V_2 measured by the probe or by the rotated probe and $\psi(\eta)$ is a proper phase function. The error occurring when $\tilde{V}(\eta)$ is approximated by a bandlimited function, is negligible as the bandwidth exceeds a critical value W_η [14] and can be effectively controlled by choosing a bandwidth factor χ', slightly greater than unity for electrically large antennas.

According to the unified theory of spiral scanning for non-spherical antennas [17], a two-dimensional OSI expansion to reconstruct the voltage from a non-redundant number of samples collected by the probe along a spherical spiral can be obtained: a) by developing a non-redundant sampling representation of the probe voltage on the spiral; b) by choosing the spiral step equal to the sample spacing required to interpolate the data along a meridian. In particular, having adopted an oblate ellipsoid as AUT modelling, the bandwidth W_η and parameterization η relevant to a meridian, and the corresponding phase function ψ are [12, 14]:

$$W_\eta = (4a/\lambda)\, E(\pi/2|\varepsilon^2)\,, \tag{2}$$

$$\eta = (\pi/2)\left[E\left(\sin^{-1}u\,|\,\varepsilon^2\right)\Big/E\left(\pi/2\,|\,\varepsilon^2\right)\right]\,, \tag{3}$$

$$\psi = \beta a\left[v\sqrt{\frac{v^2-1}{v^2-\varepsilon^2}} - E\left(\cos^{-1}\sqrt{\frac{1-\varepsilon^2}{v^2-\varepsilon^2}}\;\Big|\;\varepsilon^2\right)\right]\,, \tag{4}$$

wherein λ is the wavelength, β is the wavenumber, $u = (r_1 - r_2)/2f$ and $v = (r_1 + r_2)/2a$ are the elliptic coordinates, $r_{1,2}$ being the distances from observation point P to the foci of the ellipse C' (intersection curve between a meridian plane and Σ) and $2f$ its focal distance. Moreover, $\varepsilon = f/a$ is the eccentricity of C' and $E(\bullet\,|\,\bullet)$ denotes the elliptic integral of second kind. It is worth noting that, in any meridian plane, the curves ψ = const and η = const are ellipses and hyperbolas confocal to C' [17].

According to [12, 17], the spiral is obtained by projecting onto the scanning sphere (via the curves at η = const) a proper spiral that wraps Σ and, according to the previous discussion, the step of this projecting spiral must be equal to the sample spacing $\Delta\eta = 2\pi/(2N''+1)$ needed to interpolate the voltage along a meridian. In this last relation, $N'' = \mathrm{Int}(\chi N')+1$, where $N' = \mathrm{Int}(\chi' W_\eta)+1$, $\chi > 1$ is an oversampling factor [16] which allows the control of the truncation error, and $\mathrm{Int}(x)$ denotes the integer part of x. Therefore, the parametric equations of the spherical spiral are:

$$\begin{cases} x = d\,\sin\theta(\eta)\cos\phi \\ y = d\,\sin\theta(\eta)\sin\phi \\ z = d\,\cos\theta(\eta) \end{cases}\,, \tag{5}$$

wherein ϕ is the angular parameter describing it and $\eta = k\phi = \phi/(2N''+1)$. It is worthwhile to note that the spiral angle θ, unlike the polar angle ϑ, can assume negative values. Moreover, ϕ is always continuous, whereas, according to (5), the azimuthal angle φ exhibits a discontinuity jump of π when the spiral crosses the poles.

The parameter ξ and phase factor γ to get a non-redundant representation along the spiral can be again determined by applying the unified theory [17]. In particular, γ coincides with the phase function ψ relevant to a meridian, and ξ is β/W_ξ times the arc length of the projecting point that lies on the spiral wrapping Σ. Moreover, W_ξ is chosen equal to β/π

times the length of the spiral wrapping the surface Σ from pole to pole [12, 17].

According to the above results, the reduced voltage at P on the meridian at φ can be recovered via the OSI expansion:

$$\tilde{V}(\eta(\vartheta),\varphi) = \sum_{n=n_0-q+1}^{n_0+q} \tilde{V}(\eta_n)\, \Omega_N(\eta-\eta_n)\, D_{N''}(\eta-\eta_n) \qquad (6)$$

wherein $\tilde{V}(\eta_n)$ are the intermediate samples, i.e., the reduced voltage values at the intersection points between the spiral and the meridian passing through the observation point P, $2q$ is the retained samples number, $n_0 = \mathrm{Int}[(\eta-\eta_0)/\Delta\eta]$, and

$$\eta_n = \eta_n(\varphi) = k\varphi + n\Delta\eta = \eta_0 + n\Delta\eta \qquad (7)$$

Moreover,

$$D_{N''}(\eta) = \frac{\sin((2N''+1)\eta/2)}{(2N''+1)\sin(\eta/2)} \qquad (8)$$

$$\Omega_N(\eta) = \frac{T_N\left[-1+2(\cos(\eta/2)/\cos(\bar{\eta}/2))^2\right]}{T_N\left[-1+2/\cos^2(\bar{\eta}/2)\right]} \qquad (9)$$

are the Dirichlet and Tschebyscheff sampling functions, wherein $T_N(\eta)$ is the Tschebyscheff polynomial of degree $N = N''-N'$ and $\bar{\eta} = q\Delta\eta$.

The intermediate samples $\tilde{V}(\eta_n)$ are recovered [12] via a similar OSI expansion along the spiral:

$$\tilde{V}(\xi(\eta_n)) = \sum_{m=m_0-p+1}^{m_0+p} \tilde{V}(\xi_m)\, \Omega_M(\xi-\xi_m)\, D_{M''}(\xi-\xi_m) \qquad (10)$$

where $m_0 = \mathrm{Int}(\xi/\Delta\xi)$, $2p$ is the retained samples number, and

$$\xi_m = m\Delta\xi = 2\pi m/(2M''+1) \qquad (11)$$

with $M'' = \mathrm{Int}(\chi M')+1$ and $M' = Int(\chi' W_\xi)+1$.

It is worth noting that, when interpolating the voltage in the neighbourhood of the poles ($\vartheta = 0$ and $\vartheta = \pi$), it is necessary to increase the factor χ' to avoid a significant growth of the band limitation error, since small variations of ξ correspond to very large changes of the angular parameter ϕ in these zones.

It is so possible to get the NF data needed to perform the classical NF–FF transformation with spherical scanning [5], as modified in [6, 7].

III. Description of the Experiment:

In order to demonstrate this technique and show its usefulness for automotive antenna measurements a set of measurements were planned. An antenna was chosen for testing that was reasonably well known to the authors. Hess and others have used this particular antenna to check out other measurement systems [31]. The test scenario involved a flat plate antenna array with its main beam normal to the flat plate. The measurement system chosen to test this antenna was a roll over azimuth configuration. This test scenario is similar to an automotive application for satellite reception. The main beam is perhaps somewhat narrower that what is typical for GPS reception, but is applicable to some steerable direct broadcast systems. The flat plate has a source distribution over much of the flat plate. Adequate determination of the patterns will demonstrate that in an automotive application, primary sources and secondary sources re-radiated by the vehicle surface are adequately preserved in the far-field patterns.

The antenna under test chosen for the measurement campaign is an 45.7 cm (18-in) diameter array operating at 9.375 GHz; it is linearly polarized and has first sidelobes approximately 30 dB below the main beam peak. A photograph of this antenna is shown in Figure 3. In previous work on back projection techniques, two of the elements were blocked with metalized mylar tape, as shown. These were left on the antenna for this campaign.

Data was acquired in a polar orientation similar to Figures 1 and 2. The polar orientation was achieved by pointing the aperture normal along the Z axis.

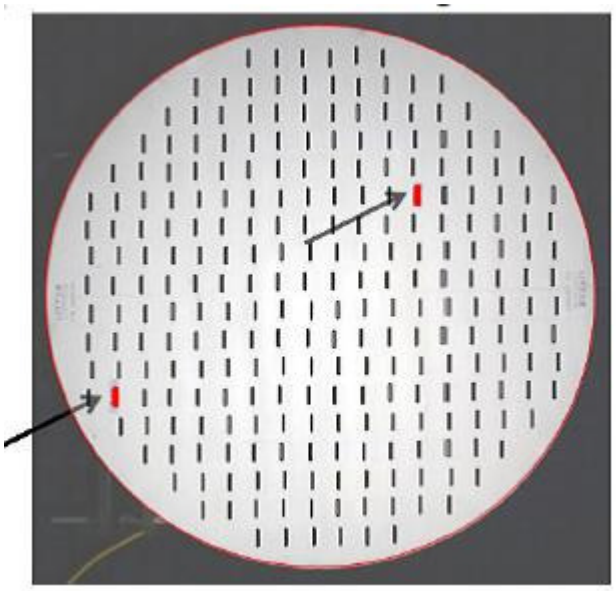

Figure 3: Overlay of Element Map and Photograph of the 45.7 cm (18 in) Flat Plate Array

Spherical spiral scanning following the method in section II was accomplished in an anechoic chamber using a roll over azimuth AUT positioner. A set of 3733 points was determined in order to acquire an optimally scanned spherical near-field spiral scan on a complete sphere. For comparison purposes a classical spherical near-field scan utilizing equally spaced data would require 7200 points.

A set of data was also acquired using MI Technologies' in-house compact range system. This system has a 1.8m cylindrical quiet zone. This system had recently been calibrated and certified for operation over its full frequency band which included the frequency of this measurement.

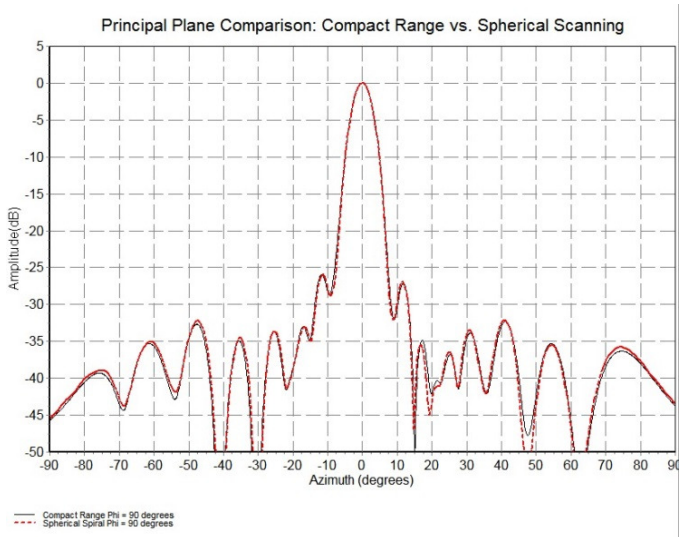

(a)

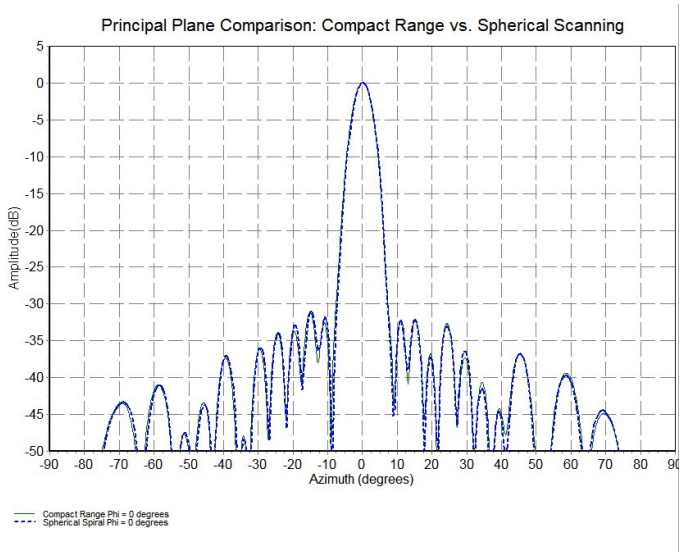

(b)

Figure 4: Comparison of the measured far-field patterns of the array. (a) E-Plane, (b) H-Plane. In both figures, the solid line represents data collected on a compact range and the dashed line represents patterns acquired via spherical spiral scanning.

Figure 4 shows the E-Plane and the H-Plane principal plane patterns of the AUT. The comparison of the two patterns taken on two different ranges utilizing two different methods is exceptional. As shown in the two figures, the equivalent stray signal computed using the method outlined in [32] is approximately -60 dB. A stray signal of this relative level would result in a +/-0.3 dB uncertainty on a -30 dB sidelobe. This value compares favorably with the compact range uncertainty analysis method proposed by Blalock et al. [30]. The uncertainty estimate for a -30 dB sidelobe level on the compact range is +/-0.54 using this method. The expected uncertainty level of the SNF measurement is +/-0.53 and was determined using the methods outlined in the IEEE Recommended Practice on Near-Field Antenna Measurements [29].

IV. Summary and Conclusions:

Spherical near-field measurements have long been used for making complex antenna measurements. The advantages of collecting measurements indoors for large test objects such as automobiles lead to the natural choice of SNF antenna measurements. Testing of antennas on automobiles is particularly challenging due to the size and weight of the test vehicle, the need for a large turntable, and often times the desire to test at lower frequencies.

Methods have been introduced to reduce the number of samples required in the near field to adequately determine the far-field patterns. These techniques involve determining the minimum number of measurement points along a spiral on a surface. Using these techniques, significant time savings can be achieved in the acquisition time required to collect a near-field measurement sample set. In order to minimize the set of samples, a source model must be chosen which takes advantage of the geometry of the AUT. For the purposes of automotive measurements, the AUT is generally assumed to be the entire vehicle and having a shape that is shorter in height than its length. This geometry is taken advantage of by following the source model presented in section II when determining the proper set of data acquisition points.

V. Acknowledgement

The authors would like to thank Andrew Bacon, Scott McBride and Fernando Nelson for contributing to the collection and processing of the measured data used in the analysis.

VI. References

[1] A.D. Yaghjian, "An overview of near-field antenna measurements," *IEEE Trans. Antennas Prop.*, vol. AP-34, pp. 30-45, Jan. 1986.

[2] J. Appel-Hansen, J.D. Dyson, E.S. Gillespie, and T.G. Hickman, "Antenna measurements," chapter 8 in *The Handbook of Antenna Design*, A.W. Rudge, K. Milne, A.D. Olver, and P.Knight, (eds.), London, UK, Peter Peregrinus, 1986.

[3] E.S. Gillespie (ed.), "Special issue on near-field scanning techniques," *IEEE Trans. Antennas Prop.,* vol. AP-36, pp. 727-901, June 1988.

[4] M.H. Francis (ed.), IEEE Recommended Practice for Near-Field Antenna Measurements, IEEE Standard 1720-2012.

[5] C. Gennarelli, A. Capozzoli, L. Foged, J. Fordham, and D.J. van Rensburg (Eds.), "Special issue on recent advances in near-field to far-field transformation techniques," *Int. J. Antennas Prop.*, vol. 2012.

[6] P.F. Wacker, Non-planar near-field measurements: Spherical scanning, NBSIR 75-809, Boulder, CO, 1975.

[7] F.H. Larsen, "Probe correction of spherical near-field measurements," Electr. Lett, vol. 13, pp. 393–395, July 1977.

[8] A.D. Yaghjian and R.C. Wittmann, "The receiving antenna as a linear differential operator: application to spherical near-field measurements," IEEE Trans. Antennas Prop., vol. AP-33, pp. 1175-1185, Nov. 1985.

[9] J.E. Hansen and F. Jensen, "Spherical Near-Field Scanning at the Technical University of Denmark," IEEE Trans. Antennas Prop., vol. AP-36, pp. 734-739, June 1988.

[10] J. Hald, J.E. Hansen, F. Jensen, and F.H. Larsen, Spherical near-field antenna measurements, J.E. Hansen, Ed. London: Peter Peregrinus, 1988.

[11] T.B. Hansen, "Higher-order probes in spherical near-field scanning," IEEE Trans. Antennas Prop., vol. 59, pp. 4049-4059, Nov. 2011.

[12] O.M. Bucci, C. Gennarelli, G. Riccio, and C. Savarese, "Data reduction in the NF–FF transformation technique with spherical scanning," Jour. Electromagn. Waves Appl., vol. 15, pp. 755-775, June 2001.

[13] F. D'Agostino, F. Ferrara, C. Gennarelli, R. Guerriero, and M. Migliozzi, "Effective antenna modellings for a NF–FF transformation with spherical scanning using the minimum number of data," Int. Jour. Antennas Prop., vol. 2011, ID 936781, 11 pages.

[14] R.G. Yaccarino, L.I. Williams, and Y. Rahmat-Samii, "Linear spiral sampling for the bipolar planar antenna measurement technique," IEEE Trans. Antennas Prop., vol. AP-44, pp. 1049-1051, July 1996.

[15] O.M. Bucci, F. D'Agostino, C. Gennarelli, G. Riccio, and C. Savarese, "NF–FF transformation with spherical spiral scanning," IEEE Antennas Wireless Prop. Lett., vol. 2, pp. 263-266, 2003.

[16] F. D'Agostino, C. Gennarelli, G. Riccio, and C. Savarese, "Theoretical foundations of near-field–far-field transformations with spiral scannings," Prog. in Electr. Res., vol. PIER 61, pp. 193-214, 2006.

[17] F. D'Agostino, F. Ferrara, C. Gennarelli, R. Guerriero, M. Migliozzi, and G. Riccio, "A nonredundant near-field to far-field transformation with spherical spiral scanning for nonspherical antennas," The Open Electrical & Electronic Eng. Jour., vol. 3, pp. 4-11, 2009.

[18] F. D'Agostino, F. Ferrara, C. Gennarelli, R. Guerriero, and M. Migliozzi, "Far–field reconstruction from a minimum number of spherical spiral data using effective antenna modellings," Prog. in Electr. Res. B, vol. 37, pp. 43-58, 2012.

[19] O.M. Bucci, C. Gennarelli, and C. Savarese, "Representation of electromagnetic fields over arbitrary surfaces by a finite and non redundant number of samples," IEEE Trans. Antennas Prop., vol. 46, pp. 351-359, March 1998.

[20] O.M. Bucci and C. Gennarelli, "Application of nonredundant sampling representations of electromagnetic fields to NF-FF transformation techniques," Int. Jour. Antennas Prop., vol. 2012, ID 319856, 14 pages.

[21] O.M. Bucci, C. Gennarelli, and C. Savarese, "Optimal interpolation of radiated fields over a sphere," IEEE Trans. Antennas Prop., vol. AP-39, pp. 1633-1643, Nov. 1991.

[22] F. D'Agostino, F. Ferrara, C. Gennarelli, R. Guerriero, and M. Migliozzi, "The unified theory of near–field – far–field transformations with spiral scannings for nonspherical antennas," Prog. in Electr. Res. B, vol. 14, pp. 449-477, 2009.

[23] F. D'Agostino, F. Ferrara, J.A. Fordham, C. Gennarelli, R. Guerriero, and M. Migliozzi, "An experimental validation of the near-field - far-field transformation with spherical spiral scan," IEEE Antennas Prop. Mag., vol. 55, no. 3, pp. 228-235, 2013.

[24] F. D'Agostino, F. Ferrara, C. Gennarelli, R. Guerriero, and M. Migliozzi, "Experimental assessment of an effective near-field - far-field transformation with spherical spiral scanning for quasi-planar antennas," IEEE Antennas Wireless Prop. Lett., vol. 12, pp. 670-673, 2013.

[25] F. D'Agostino, F. Ferrara, C. Gennarelli, R. Guerriero, and M. Migliozzi, "Far-field reconstruction from near-field data acquired via a fast spherical spiral scan: experimental evidences," Prog. in Electr. Res., vol. 140, pp. 719-732, 2013.

[26] F. D'Agostino, F. Ferrara, C. Gennarelli, R. Guerriero, and M. Migliozzi, "Experimental testing on an effective technique to reconstruct the far-field pattern of a long antenna from near-field measurements acquired via spherical spiral scan," The Open Electrical & Electronic Eng. Jour., vol. 8, pp. 1-9, 2014.

[27] Efficient reconstruction of the pattern radiated by a long antenna from data acquired via a spherical spiral scanning near-field facility," IEEE Antennas Prop. Mag., vol. 56, no. 2, pp. , 2014

[28] O.M. Bucci, G. D'Elia, and M.D. Migliore, "Advanced field interpolation from plane-polar samples: experimental verification," IEEE Trans. Antennas Prop., vol. 46, pp. 204-210, Feb. 1998.

[29] IEEE Standard 1720-2012 Recommended Practices for Near-Field Antenna Measurements.

[30] S. Blalock, D. Wayne, and J.A. Fordham, "Estimating Measurement Uncertainties in Compact Range Antenna Measurements." Proceedings of the Antenna Measurement Technique Association, 2015

[31] D. Hess and S. McbBride, "Back-Projection to the Aperture of a Planar Phased Array from Data Obtained with a Spherical Near-Field Arch" Proceedings of the Antenna Measurement Technique Association, 2009

[32] J. Fordham and M. Scott, "Antenna Pattern Comparison Between an Outdoor Cylindrical Near-Field Test Facility and an Indoor Spherical Near-Field Test Facility," IEEE Antennas Prop. Mag., vol. 46, no. 3, June 2004